BioControl (2016) 61:269–282
DOI 10.1007/s10526-015-9706-z

Fate of *Trichoderma harzianum* in the olive rhizosphere: time course of the root colonization process and interaction with the fungal pathogen *Verticillium dahliae*

David Ruano-Rosa · Pilar Prieto · Ana María Rincón · María Victoria Gómez-Rodríguez · Raquel Valderrama · Juan Bautista Barroso · Jesús Mercado-Blanco

Received: 2 June 2015 / Accepted: 3 November 2015 / Published online: 7 November 2015

Abstract *Trichoderma harzianum* Rifai is a well-known biological control agent (BCA) effective against a wide range of phytopathogens. Since colonization and persistence in the target niche is crucial for biocontrol effectiveness we aimed to: (i) shed light on the olive roots colonization process by *T. harzianum* CECT 2413, (ii) unravel the fate of its biomass upon application, and (iii) study the *in planta* interaction with the soil-borne pathogen *Verticillium dahliae* Kleb. Fluorescently-tagged derivatives of CECT 2413 and *V. dahliae* and confocal laser scanning microscopy were used. In vitro assays showed for the first time mycoparasitism of *V. dahliae* by *T. harzianum*, evidenced by events such as hyphal coiling. *In planta* assays revealed that CECT 2413 profusely colonized the rhizoplane of olive roots. Interestingly, biomass of the BCA was visualized mainly as chlamydospores. This observation was independent on the presence or absence of the pathogen. Evidence of inner colonization of olive roots by CECT 2413 was not obtained. These results suggest that CECT 2413 is not able to persist in a metabolically-active form when applied as a spore suspension. This may have strong implications in the way this BCA should be introduced and/or formulated to be effective against Verticillium wilt of olive.

Keywords Chlamydospores · Confocal laser scanning microscopy · Mycoparasitism · *Olea europaea* L. · *Trichoderma harzianum* Rifai · Root colonization · *Verticillium dahliae* Kleb. · Verticillium wilt

Handling Editor: Monica Hofte.

D. Ruano-Rosa · J. Mercado-Blanco (✉)
Laboratory of Plant-Microorganism Interaction, Department of Crop Protection, Institute for Sustainable Agriculture, Agencia Estatal Consejo Superior de Investigaciones Científicas (CSIC), C/Alameda del Obispo s/n, CP 14080, Córdoba, Spain
e-mail: jesus.mercado@ias.csic.es

P. Prieto
Department Plant Breeding, Institute for Sustainable Agriculture, Agencia Estatal Consejo Superior de Investigaciones Científicas (CSIC), Córdoba, Spain

A. M. Rincón
Department of Genetics, Faculty of Biology, University of Seville, Seville, Spain

M. V. Gómez-Rodríguez · R. Valderrama · J. B. Barroso
Group of Biochemistry and Cell Signalling in Nitric Oxide, Department of Experimental Biology, Center for Advanced Studies in Olive Grove and Olive Oils, University of Jaén, Jaén, Spain

Introduction

A growing social demand for agricultural products free of harmful compounds for both human and animal health and for the environment has encouraged the research on biological control agents (BCA) as an alternative to chemical-based products for effective

crop diseases management. Among microorganisms studied and employed as BCA, species of the filamentous fungal genus *Trichoderma* arise as one of the most outstanding. *Trichoderma* spp. are thus considered the BCA par excellence among fungi due to: (i) their well-documented antimicrobial activity, consequence of mechanisms (not mutually exclusive) such as antibiosis, mycoparasitism and/or competition (Harman and Kubicek 1998; Verma et al. 2007); (ii) their ability to induce systemic resistance (Harman et al. 2004; Contreras-Cornejo et al. 2013); and/or (iii) their positive effects on seed germination and plant growth (e.g. Hermosa et al. 2012). Moreover, *Trichoderma* spp. are highly versatile and show cosmopolitan distribution (Druzhinina et al. 2011; Kredics et al. 2014). Taking into account all these characteristics, *Trichoderma* spp. are widely selected as BCA against soil-borne pathogens (e.g. Ruano-Rosa et al. 2010; 2014), and constitute the base of many registered bioformulations worldwide (Verma et al. 2007; Lorito and Woo 2015). Even though our knowledge on mechanisms underlying biocontrol exerted by *Trichoderma* spp. is abundant, there is still an important lack of information on how *Trichoderma* spp. interact with the host plant and the target phytopathogen in a scenario such as the rhizosphere, where multiple trophic interactions take place (Raaijmakers et al. 2009). Research pursuing this aim is scant and therefore needed to better understand the fate of this BCA once applied to roots or soil, especially in the case of woody plants with large root systems.

Trichoderma harzianum Rifai is employed as BCA against a wide range of plant pathogens, such as *Fusarium oxysporum* f. sp. *phaseoli* (Carvalho et al. 2014). *Trichoderma harzianum* CECT 2413 is a well-documented isolate of this genus due to its demonstrated mycoparasitic activity against different pathogens, for instance *Rhizoctonia meloni* and *Phytophthora citrophthora* (Moreno-Mateos et al. 2007), and its plant growth promotion capability (Chacón et al. 2007). Related to root colonization, CECT 2413 has mostly been studied on non-woody plants like tomato (*Solanum lycopersicum* L.) (Chacón et al. 2007), cucumber (*Cucumis sativus* L.) (Samolski et al. 2012) or *Arabidopsis thaliana* L. (Alonso-Ramirez et al. 2014).

Verticillium wilt of olive (*Olea europaea* L.) (VWO) is caused by the soil-borne fungus *Verticillium dahliae* Kleb. This disease is considered one of the most important biotic constraints for olive cultivation in many regions, particularly in the Mediterranean Basin. Unfortunately, VWO is very difficult to control and must be confronted by means of an integrated disease management (IDM) strategy (López-Escudero and Mercado-Blanco 2011). An interesting approach to control VWO in a sustainable, environment-friendly way and within IDM frameworks is by using BCA, particularly at the nursery production stage (Tjamos 1993). So far, however, only a few reports have demonstrated the effectiveness of BCA against VWO (Mercado-Blanco et al. 2004; Prieto et al. 2009), identified a number of taxa with potential to control *V. dahliae* (Papasotiriou et al. 2013), or used promising combinations of BCA and organic amendments (Vitullo et al. 2013). *Trichoderma* spp. have also been investigated either on their potential to antagonize *V. dahliae* in nurseries potting mixes (Aleandri et al. 2015), or as bioformulations against VWO caused by the defoliating (D) pathotype of *V. dahliae* (Jiménez-Díaz et al. 2009). Recently, the use of a formulation based on *T. harzianum* CECT 2413 to control VWO has been patented and licensed (Spanish patent number ES 2393728 A1, Barroso Albarracín et al. 2014). Isolate CECT 2413 has been demonstrated to be an effective in vitro antagonist against different isolates of *V. dahliae*, as well as able to control VWO caused by the D pathotype under controlled conditions and to promote olive growth (Barroso Albarracín et al. 2014; Rincón et al. 2014).

Under specific conditions *V. dahliae* and *Trichoderma* spp. can develop resistant structures, enabling them to survive under adverse conditions. Thus, *V. dahliae* produce microsclerotia (MS), melanized structures mainly produced at the end of the parasitic phase of its life's cycle and able to endure in soils for a prolonged period of time (Pegg and Brady, 2002). On the other hand, many species of the genus *Trichoderma* develop chlamydospores (globose or ellipsoidal, intercalary or terminal, smooth-walled, yellowish, greenish or without colour, and with diameter between 6 and 15 μm) (Cohen et al. 1983).

A key prerequisite to achieve effective biocontrol by any artificially-introduced BCA is the efficient colonization of the target niche. The BCA must thus be able to rapidly colonize the working site and to adapt and endure the harsh (a)biotic conditions that they likely have to face after being released. However, this is not always the case and there is an important lack of

knowledge on the fate that a BCA undergoes after its introduction in a new environment. A number of uncertainties still need to be tackled to better understand why a BCA is not always able to behave in the way it is expected. Regarding to the tripartite interaction olive-*Trichoderma*-*V. dahliae* nothing is known.

The specific objectives of this study were: (i) to study, at the microscopic level, the interaction between *T. harzianum* CECT 2413 and *V. dahliae* D pathotype under in vitro and *in planta* conditions, (ii) to determine the olive roots colonization process by CECT 2413 over time, and (iii) to check whether isolate CECT 2413 is able to colonize endophytically olive root tissues. We have aimed to better understand the behavior of this BCA in the olive rhizosphere in the absence and presence of one of the most devastating soil-borne pathogens affecting this woody crop.

Materials and methods

Fungal isolates

A green fluorescent protein (GFP)-labeled derivative of *T. harzianum* CECT 2413 (*Th*-GFP; Chacón et al. 2007) and the enhanced yellow fluorescent protein (EYFP)-labeled derivative of *V. dahliae* V937I D (isolate VDAT-36I; Prieto et al. 2009) were used in this study. They were maintained at −80 °C and recovered when needed on potato dextrose agar (PDA; Oxoid Ltd, Hampshire, UK).

In vitro interaction of *Th*-GFP and VDAT-36I

In order to examine the interaction between fluorescently-labeled derivatives of isolate CECT 2413 and *V. dahliae* V937I, an experimental setup enabling microscopy observation was designed. Sterile excavated microscope slides were prepared by filling the concavities (15 mm diameter) with a thin layer of PDA. Then, both fungi were deposited by gently touching with sterile toothpicks of which the tips were immersed in saturated conidial suspensions of each fungus (*Th*-GFP and VDAT-36I). The distance between both fungi was 1 cm (Fig. 1a). Slides were carefully deposited within sterile, sealed Petri dishes and incubated during 72 h at 25 °C in the dark. The slides (5) were observed by confocal laser scanning microscopy (CLSM) at 24, 48 and 72 h after inoculation of the fungi with an Axioskop 2 MOT microscope (Carl Zeiss, Jena GmbH, Germany) equipped with a Krypton and an Argon laser, controlled by Carl Zeiss Laser Scanning System LSM5 PASCAL software (Carl Zeiss, Jena GmbH, Germany). Enhanced *Th*-GFP was exposed to 488 nm Argon laser light (detection at 500–520 nm), and the EYFP-labeled VDAT-36I to 514 nm Argon laser light (emission 530–620). The same expositions were used for *in planta* tripartite interaction experiments (see below). Data were recorded and the images transferred for analysis to Zeiss LSM Image Browser version 4.0 (Carl Zeiss, Jena GmbH, Germany). Images were processed with Photoshop CS6 (Adobe Systems Inc., San Jose, California, USA).

Time course of early and long-term colonization events of olive roots by *T. harzianum* CECT 2413

A bioassay was performed with the aim to obtain detailed observations of the colonization process in olive roots by the fluorescently-tagged derivative *Th*-GFP. A single application of pre-germinated conidia of *Th*-GFP was performed using the following procedure. Petri dishes containing PDA were inoculated with a mycelial disk (5 mm diameter) and incubated at 25 °C in the dark during five days. Then, 5 ml of sterile distilled water were added to each plate and the conidia were scraped and filtered by sterile chiffon. This conidia suspension was used to inoculate Petri dishes of PDA (100 µl per plate). The plates were incubated until profuse conidiation (25 °C in the dark; seven days), processed in the same way as described above to obtain the conidia suspension, and quantified by using a haemocytometer. The inocula concentration was adjusted as necessary. Conidia were germinated on potato dextrose broth (33 %) (PDB; Oxoid Ltd, Hampshire, UK) by incubating in an orbital shaker (200 rpm) during 15 h at 25 °C in the dark. Conidia germination was corroborated by light microscope (Nikon YS100, Nikon Corp., Tokyo, Japan) and the medium was eliminated by centrifugation (4400 rpm, 10 min; Eppendorf centrifuge 5804 R, Germany) and three washes with sterile distilled water. Pre-germinated conidia were suspended in sterile distilled water and quantified again using a haemocytometer. The experiment was conducted using ten-month olive plants of the VWO susceptible

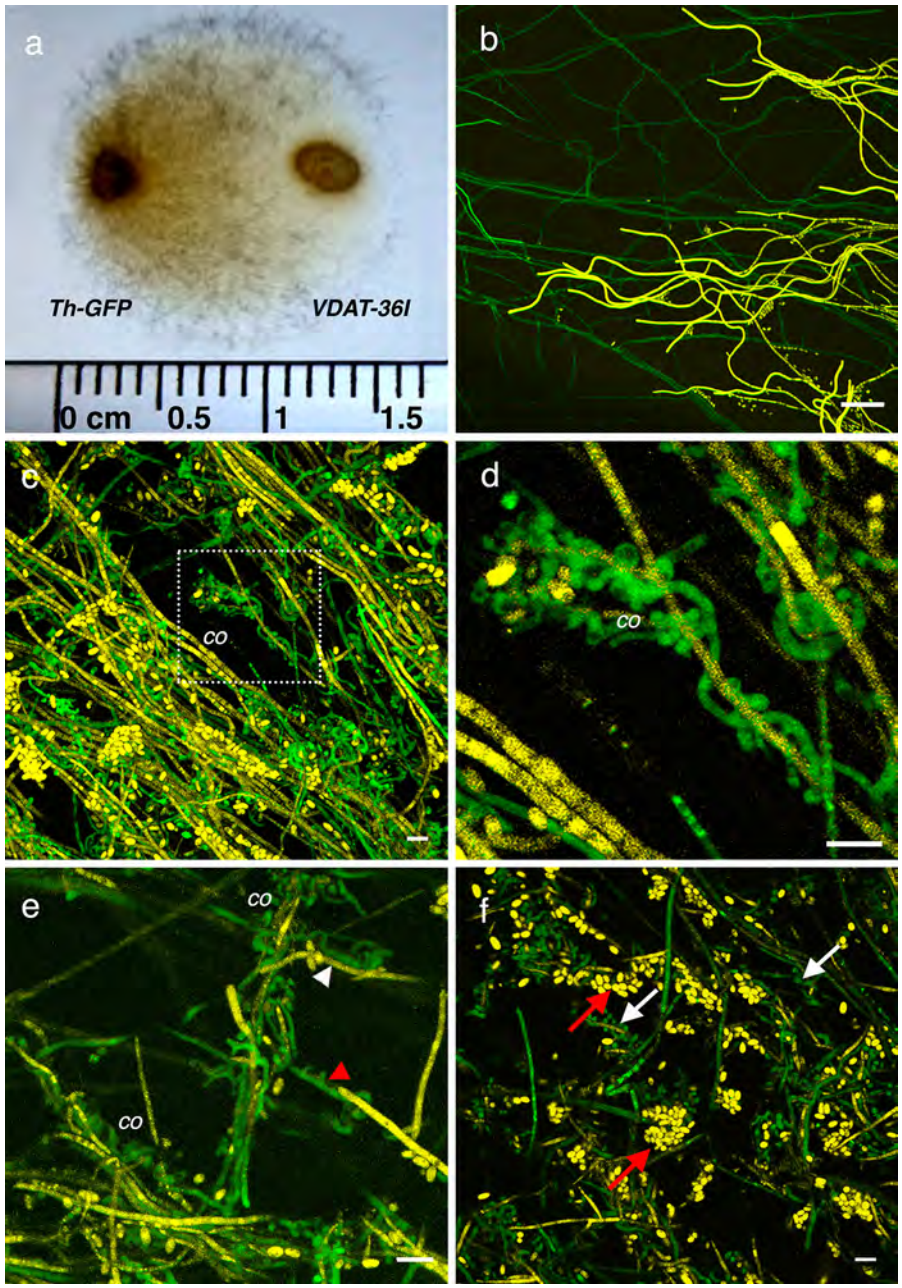

Fig. 1 In vitro analysis of the interaction between fluorescently-labeled derivatives of *Trichoderma harzianum* CECT 2413 (*Th*-GFP) and a defoliating representative of the soil-borne pathogen *Verticillium dahliae* (VDAT-36I) using confocal laser scanning microscopy. Dual cultures were incubated (25 °C, 72 h) in excavated microscope slides filled in with potato-dextrose-agar medium. **a** Macroscopic view of the experimental setup 72 h after inoculation. Fungi were inoculated at a distance of 1 cm. **b** Intermingled growth of *Th*-GFP (*green*) and VDAT-36I (*yellow*) hyphae observed at 48 h after inoculation. **c**–**e** Hyphae of *Th*-GFP (*green*) forming coils wrapping VDAT-36I hyphae (*yellow*) observed at 72 h. Papilla-like (*white arrowhead*) and hook-like (*red arrowhead*) structures were observed together with degradation of VDAT-36I mycelia (*red arrowhead*). Panel **d** shows the inset indicated by a *dashed-line square* in panel **c**. **f** Asexual reproductive structures of *Th*-GFP (*white arrows*) and VDAT-36I (*red arrows*). Bars represent 10 μm in all panels except in **b** where it represents 50 μm. (*co*) coiling. (Color figure online)

cv. Picual (López-Escudero et al. 2004) originated from a commercial nursery in Córdoba province (Southern Spain). The roots were carefully washed under tap water avoiding intentional wounding, and dipped in a suspension of 2×10^5 *Th*-GFP pre-germinated conidia ml^{-1} prepared in minimal medium (MM) (Penttilä et al. 1987) amended with 0.2 % (w/v) glycerol as sole carbon source and 20 mg l^{-1} of ammonium sulphate (Chacón et al. 2007). Plants with their root systems immersed in this suspension were then placed in an orbital shaker (100 rpm) (Comecta SA 200-D, JP Selecta Group, Barcelona, Spain) within a growth chamber at 24 ± 1 °C in the dark and 60–70 % RH. After 12 h, the plants were transplanted to pots with sterilized perlite and placed into a growth chamber with the same conditions described above, but with a 14-h photoperiod of fluorescent light (360 mE m^{-2} s^{-1}) until the end of the experiment (109 days). Plants were watered as needed, and fertilized weekly with 50 ml per pot of Nipofol-K Plus 12-4-36 + microelements (1 g l^{-1}) (Fercampo, Málaga, Spain). For this experiment, 25 plants per treatment (i.e. un-inoculated control and *Th*-GFP) were used. Microscope observations were performed 1, 2, 3, 7, 14, 21, 29, 90, 101 and 109 days after inoculation (DAI) collecting at least two plants per day. Samples consisted in root segments (aprox. 1 cm long) carefully washed with sterile distilled water. Longitudinal and transversal sections of root segments (50 µm width) were obtained using a Vibratome (VT1000 S, Leica, Wetzlar, Germany). Additionally, secondary roots were taken and visualized without tissue sectioning. Root sections were stained with 10 µM propidium iodide (Sigma, Madrid, Spain) during 10 min to label the plant cell walls. Samples from this bioassay were analyzed with a CLSM Microscope (SP5 II, Leica, Wetzlar, Germany) using the LAS AF software (Leica Microsystems Inc., Wetzlar, Germany). Images were processed with Photoshop CS6.

Time course of interaction events of *Th*-GFP and VDAT-36I on olive roots

For assessment of the pathogen-BCA-olive interaction, inoculations with *Th*-GFP, VDAT-36I or *Th*-GFP + VDAT-36I were performed following the same procedure described above for *T. harzianum* with some differences. Plant root systems were dipped in MM modified as cited above containing 10^6 pre-germinated conidia ml^{-1} of *Th*-GFP and placed in an orbital shaker (100 rpm) into a growth chamber (Percival SA 200-D, JP Selecta Group, Barcelona, Spain) at 24 ± 1 °C in the dark and 60–70 % RH. After 12 h, the plants were transferred into new containers with a solution of MM modified with 5×10^6 pre-germinated conidia ml^{-1} of VDAT-36I during 30 min. A group of control plants were only dipped in MM modified. Plants were then transplanted to pots with sterilized soil (peat:sand:loan, 1:1:2) and placed into a growth chamber with the same conditions described above but with a 14-h photoperiod with fluorescent light (360 mE m^{-2} s^{-1}) until the end of the experiment (21 days). Plants were watered as needed, and fertilized weekly. For this experiment, 18 plants per treatment (i.e. un-inoculated control, *Th*-GFP, VDAT-36I and *Th*-GFP + VDAT-36I) were inoculated.

Root tissue samples consisted in sections of about 1 cm length from the whole root (one plant per treatment and per time-point), carefully washed with distilled water to remove residual substrate. Microscope observations were performed 1, 2, 3, 7, 10, 14, 17 and 21 DAI and carried out using the CLSM cited previously for in vitro assay. Images were also processed with Photoshop CS6.

Viability of *Th*-GFP was checked at the end of the experiment. Rhizosphere soil was thus analyzed by using a *Trichoderma* selective medium (TSM) (Askew and Laing 1993). Three replicate per plant and two plants per treatment were used. Colony forming units (CFU) per g of soil were counted after incubation during four days at 25 °C in the dark. Fluorescence of the colonies was checked using a Nikon Eclipse 80i epifluorescence microscope (Nikon UK Ltd, Surrey, UK) to rule out that indigenous *Trichoderma* spp. were present. Data means and standard deviations were calculated.

Results

In vitro interaction between *Th*-GFP and VDAT-36I

Dual cultures of the pathogen and *Th*-GFP performed on excavated microscopy slides were prepared (Fig. 1a). CLSM observations performed at 24 h

revealed that hyphae of both fungi rapidly grew until they established contact and intermingled (Fig. 1b). Evidence suggesting the existence of antibiosis was not found. Thereafter, events associated with mycoparasitism were observed. Growth of *Th*-GFP over VDAT-36I mycelium was observed at 72 h (Fig. 1a). CLSM imagery revealed that this overgrowth was accompanied by numerous events of coiling (*Th*-GFP hyphae wrapping VDAT-36I hyphae) (Fig. 1c–e; '*co*'). Other structures associated to this process such as papilla-like (Fig. 1e; white arrowhead) or hook-like (Fig. 1e; red arrowhead) structures were identified. Papilla-like structures consisted in growth and subsequence thickening of *Th*-GFP vegetative hyphae alongside VDAT-36I hyphae, while hook-like structures were identified in *Th*-GFP hyphae attached to *V. dahliae* hyphae as short lateral hyphal branches. A loss of *Verticillium* mycelium fluorescence in that point was observed (Fig. 1e; red arrowhead). Furthermore, abundant asexual reproductive structures of both fungi (i.e. conidia) were found (Fig. 1f; white and red arrows for *Th*-GFP and VDAT-36I, respectively). On the contrary, *Th*-GFP chlamydospores (globose, smooth-walled with an average diameter between 5.0 and 7.5 µm) were detected sporadically, mostly found at the end of short lateral branches of vegetative hyphae (data not shown). Concerning VDAT-36I, formation of MS was not observed during the experiment in contrast to the high number of conidia detected (Fig. 1f; red arrows).

Time course of early and long-term colonization events of olive roots by *Th*-GFP

Visualization of *Th*-GFP biomass using CLSM was evident soon after artificial inoculation of olive roots by the BCA. *Th*-GFP pre-germinated conidia were clearly observed over the olive root surface one DAI (Fig. 2a; '*g*'). However, neither evidence of penetration through the root epidermis nor preferential colonization sites were found at this time point. As early as 2 DAI, first evidence of chlamydospore development was obtained as revealed by appearance of slight hyphae swellings (Fig. 2b; yellow arrows). Moreover, conidiophores were clearly visible as well (Fig. 2b; white asterisks). Mycelium layers appeared profusely covering large surfaces of both principal and secondary roots after three days (Fig. 2c). At this moment, conidia were also visualized intermingled with mycelia and attached to the rhizoplane. First fully developed chlamydospores also appeared at this time point (3 DAI) at both intercalary (Fig. 2c, inset; white arrow) and distal positions (Fig. 2c, inset; red arrow). At 7 DAI showed little or a total absence of fluorescent mycelium/hyphae. The vast majority of the *Th*-GFP biomass visualized over the root surface, including root hairs, consisted of conidia and chlamydospores firmly attached to the epidermis (Fig. 2d, e; '*c*' and '*ch*'). No major changes were observed at 14 DAI compared to the previous time point: scarcity of mycelium, high number of conidia attached to the root surface, and chlamydospores differing neither in size nor in abundance over the rhizoplane (Fig. 2f, g; '*c*' and '*ch*'). At 21 DAI, chlamydospores were the most abundant fungal structure, covering large areas of the olive root epidermis (Fig. 2h). Fluorescent hyphae were observed for the last time in this experiment at this sampling time, although in very few spots (Fig. 2i; '*h*'). No significant changes on appearance, abundance and distribution of *Th*-GFP structures and biomass were observed over olive root surface at 29 DAI (Fig. 2j). From this time point on, plants were kept under the same conditions to gain information about the fate of *Th*-GFP biomass at long-term stages after

Fig. 2 In vivo confocal laser scanning microscopy analysis of olive (cv. Picual) roots colonization by a GFP-labeled *Trichoderma harzianum* CECT 2413 (*Th*-GFP). Three types of root tissue samples were used: longitudinal (**a**, **b**, **d–f**, **i–l**) and transversal (**g**) vibratome sections (50 µm width), and secondary roots without sectioning (**c**, **h**). All samples were stained with 10 µM Propidium-iodide. **a** Pre-germinated conidia and hyphal growth on root surface one day after inoculation (DAI). **b** Hyphal growth two DAI where first evidences of chlamydospore development appears as hyphal swelling (*yellow arrows*). *Asterisks* indicate conidiophores, asexual reproduction structures. **c** Hyphae are observed covering large portions of the root surface at three DAI. First chlamydospores are observed in terminal and intercalary positions (*inset*: *red* and *white arrows*, respectively). **d, e** chlamydospores appear as the predominant fungal structure on the root surface at seven DAI. Conidia still appear in large number while hyphae begin to disappear. **f**, **g** at 14 DAI Conidia and chlamydospores of *Th*-GFP were found surrounding root hairs. **h**, **i** Extensive colonization of the root surface after 21 DAI, mainly as conidia and chlamydospores. Progressive loss of hyphae fluorescence was observed. **j** Prevalence of chlamydospores and conidia after 29 DAI with complete absence of fluorescent hyphae. **k**, **l** Chlamydospores and conidia, but no fluorescent hyphae in the rhizoplane at 101 DAI. Black arrow (**k**) points to a chlamydospore with two cells. Bars represent 10 µm in panels **g** and **k**, 30 µm in **a**, **b**, **d**, **e**, **f**, **i**, **j** and **l**, 100 µm in **c** and **h**. *c* conidia, *ch* chlamydospore, *g* germinated conidia, *h* hyphae, *r* root, *rh* root hair. (Color figure online)

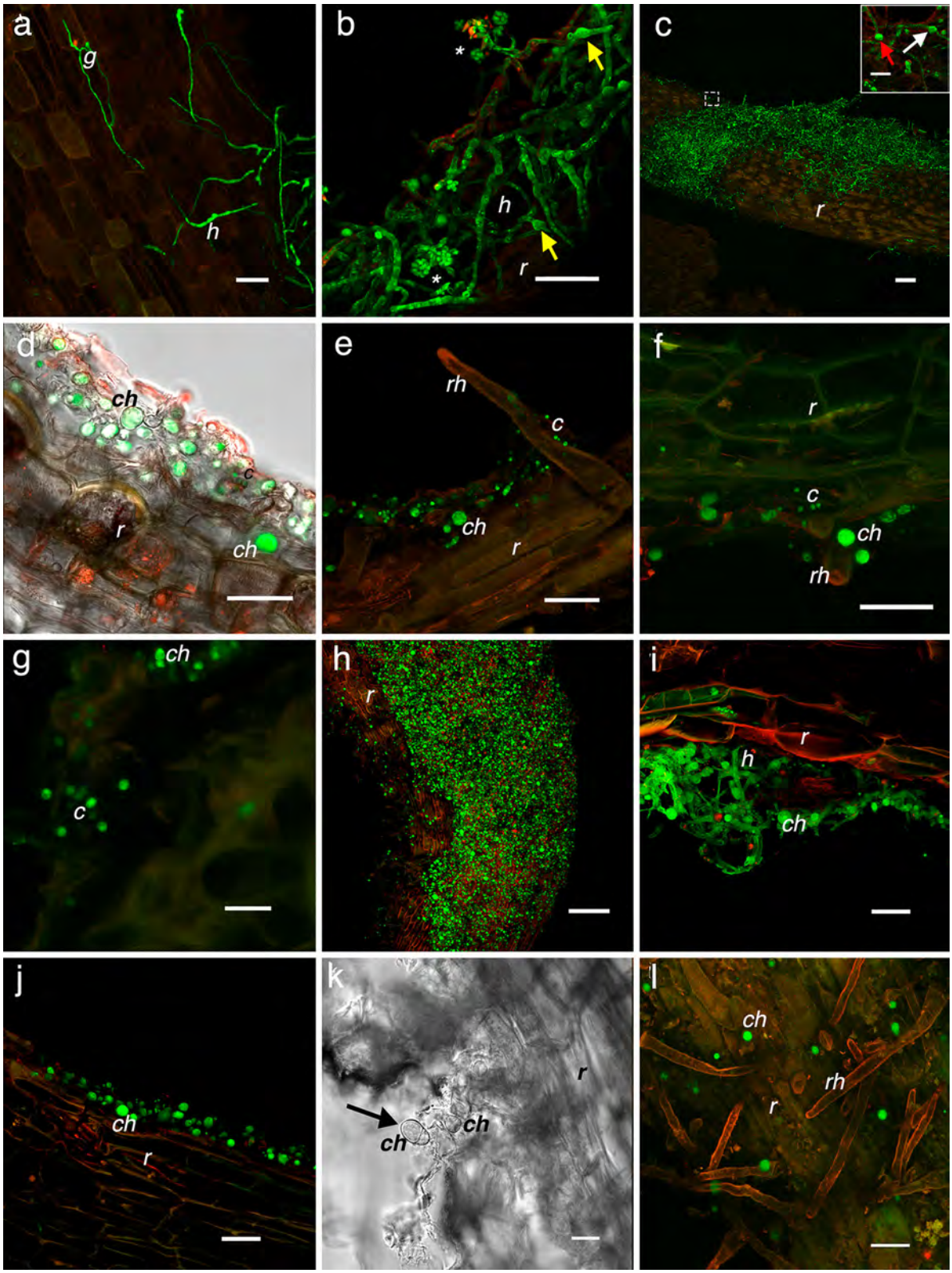
a
g
h
b
*
h
r
*
c
r
d
ch
c
r
ch
e
rh
c
ch
r
f
r
c
ch
rh
g
ch
c
h
r
i
r
h
ch
j
ch
r
k
r
ch
ch
l
ch
rh
r

inoculation (up to 100 DAI). Chlamydospores were overwhelmingly observed at this late observation times (Fig. 2k, l; '*ch*'), although their number was very low. Bicellular chlamydospores were observed (Fig. 2k; black arrow) attached to epidermis. Morphology of chlamydospores in this experiment did not differ to that generated during the in vitro experiment (i.e. globose and smooth-walled) and their average diameters were around 10 µm. Overall, hyphae of *Th*-GFP rapidly decreased over time and its biomass basically consisted of resistance structures.

Time course of early interaction events of *Th*-GFP and VDAT-36I on olive roots

To visualize how *Th*-GFP and the pathogen colonize and interact on the olive root system a similar approach was followed. A fair number of root tissue segments, representative of the whole radical system of each sampled plant, were prepared on a time-course basis and evaluated exhaustively by CLSM. At early stages (1 DAI), pre-germinated conidia of both fungi were profusely detected over the root surface regardless of whether or not fungi were single-inoculated (Fig. 3a, b; '*g*') or co-inoculated (Fig. 3c; '*g*'). No preferential colonization site was observed. Noticeably, *Th*-GFP started to develop both distal (Fig. 3a, white arrow; inset 1) and intercalary (Fig. 3a, red arrow; inset 2) chlamydospores very soon after inoculation. As observed in the dual culture assay, chlamydospores were mainly found at terminal position. Overall, few conidia were observed in this experiment for both fungi. At 2 DAI, most of the *Th*-GFP biomass observed was in the form of chlamydospores, which profusely colonized and covered entire zones of the rhizoplane regardless the absence (Fig. 3d; white arrows) or presence (Fig. 3f; white arrows) of VDAT-36I. Whereas *Th*-GFP chlamydospores increased over time, hyphae and conidia decreased dramatically. Concerning the pathogen, its mycelium increased progressively as well, developing aggregates of hyphae at specific spots on the root epidermis. These structures were observed in both roots of plants inoculated only with VDAT-36I (Fig. 3e; '*ag*') and with both fungi (Fig. 3f; '*ag*'). From 7 DAI on, fluorescent hyphae of both fungi reduced drastically and were very difficult to observe, particularly for *Th*-GFP (Fig. 3g, i). In contrast, massive development of chlamydospores was evident for *Th*-GFP (Fig. 3g, i; white arrows). Moreover, production of resistance structures (MS), evidenced by hyphae aggregation and swelling, was observed for VDAT-36I over the root epidermis (Fig. 3h, i; '*m*'). At later stages (10 DAI and on) neither fluorescent hyphae nor conidia of *Th*-GFP were observed (Fig. 3j), and an overwhelming prevalence of chlamydospores was revealed at some specific spots of the root surface (Fig. 3l; white arrows). Regarding the pathogen, its biomass sharply decreased, being more difficult to visualize except for scattered MS which tended to be the prevalent structure (Fig. 3k). Overall, observation of fluorescent structures for both fungi was difficult at later days. For instance, chlamydospores were the only structure detected at 14 DAI but they usually lost fluorescence very fast. Thus, good quality CLSM images were not possible. Eventually, at 17 and 21 DAI fluorescent fungal structures were not detected. No evidence of endophytic colonization by *Th*-GFP was found along the bioassay.

Fig. 3 *In planta* interaction between *Trichoderma harzianum* CECT 2413 and *Verticillium dahliae* VDAT-36I. Confocal laser scanning microscopy images showing the time-course of *in planta* colonization of olive (cv. Picual) roots of *T. harzianum* CECT 2413 (*Th*-GFP, *green*, *left panels* column), *V. dahliae* (VDAT-36I *dark yellow*, central panels column), and both fungi together (*right panels* column). *Images* show representative samples of the whole root system sampled at one (**a–c**), two (**d–f**), seven (**g–i**) and ten (**j–l**) days after inoculation. **a** Conidia and hyphae of *Th*-GFP colonizing the olive root epidermis. Development of distal (*white arrow*; *inset* **a1**) and intercalary (*red arrows*; *inset* **a2**) chlamydospores. **b** Conidia germination and hyphal growth of VDAT-36I on root surface. **c** Root surface showing little presence of *Th*-GFP chlamydospore. **d** Increasing number of chlamydospores face to an important decrease of conidia and hyphae. **e** Accumulation of VDAT-36I hyphae in root surface following a random pattern. **f** *Th*-GFP and VDAT-36I on root surface with profuse colonization by both fungi sharing the same spot. After this moment, hyphae of *Th*-GFP were no longer detected. **g** Chlamydospores around root hairs. A low number of conidia and complete absence of hyphae were observed. **h** VDAT-36I starts to develop microsclerotia. Presence of hyphae was scarce. **i** *Th*-GFP chlamydospores and VDAT-36I microsclerotia on root surface. Both fungi are occupying the same spot. After this moment, VDAT-36I hyphae were no longer detected. **j** Chlamydospores covering regions of the rhizoplane. **k** Microsclerotium. **l** High number of *Th*-GFP chlamydospores covering large regions of the root surface. Bars represent 50 µm in all panels except in **a1** and **a2** where represent 10 µm. *ag* aggregate, *c* conidia, *g* germinated conidia, *h* hypha, *m* microsclerotia, *r* root, *rh* root hair, '*white and red arrows*' indicate chlamydospores. (Color figure online)

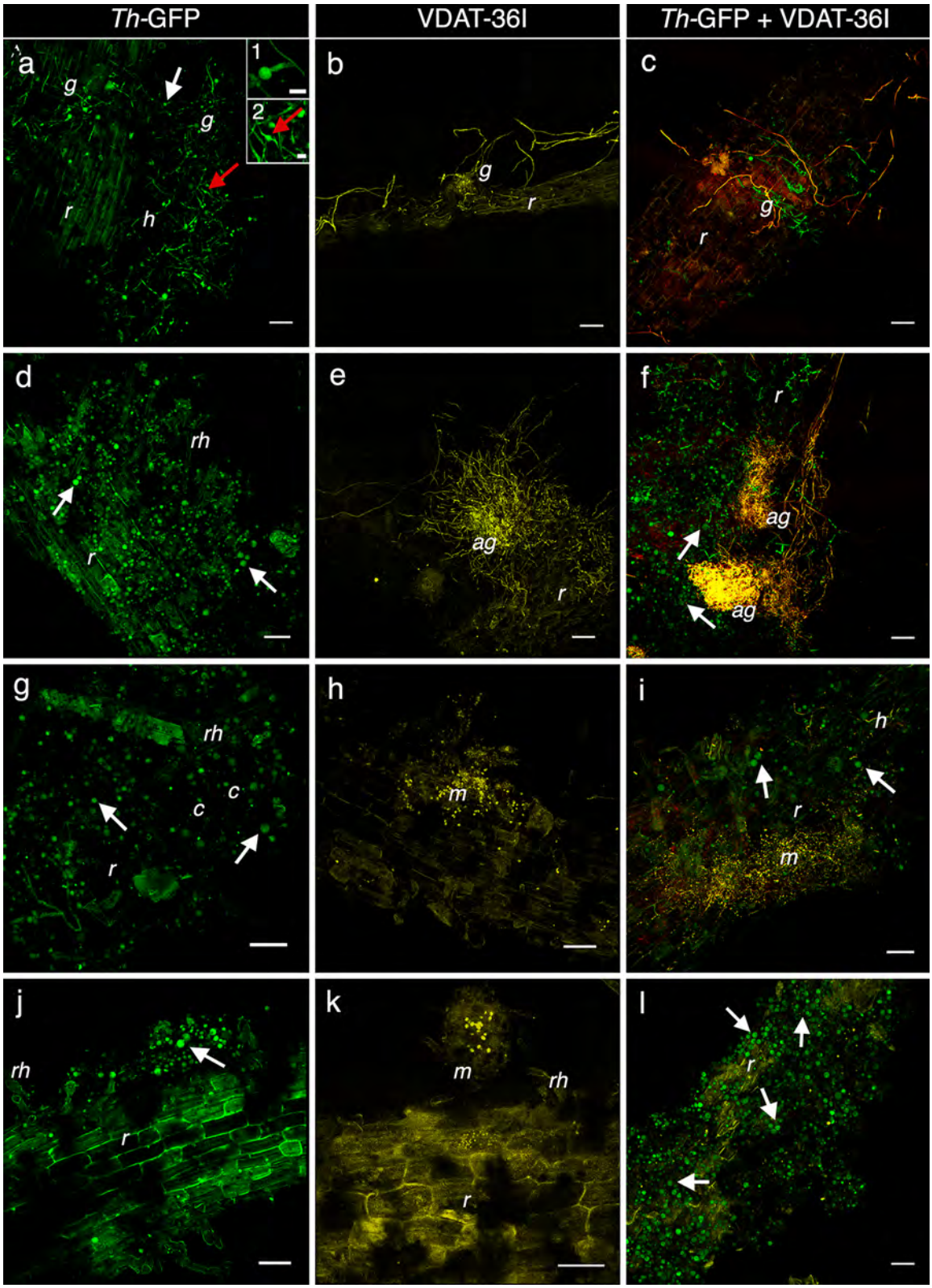
Th-GFP
VDAT-36I
Th-GFP + VDAT-36I
a
b
c
d
e
f
g
h
i
j
k
l
1
2
g
r
h
rh
ag
m
c

Finally, quantification of viable *Th*-GFP propagules at the end of the experiment yielded $1.5 \pm 0.4 \times 10^4$ and $4 \pm 0.7 \times 10^4$ cfu g^{-1} of soil in *Th*-GFP and *Th*-GFP + VDAT-36I treatments, respectively. No indigenous *Trichoderma* spp. were recovered since all grown colonies showed fluorescent under the fluorescence microscope. Likewise, no *Trichoderma* spp. were detected in the rhizosphere of un-inoculated and VDAT-36I-inoculated plants.

Discussion

The knowledge about the behavior of a given BCA when applied to the target niche (ecology) and on the interactions established with the pathogen and the host plant (trophic networks) is crucial for the successful application of BCA in agro-ecosystems. In the present study, we have proved that *T. harzianum* CECT 2413 showed mycoparasitism against *V. dahliae*, at least in vitro. Indeed, the typical events associated to this process (Chet et al. 1998) were clearly observed. Mycoparasitism is considered one of the main modes of action of *Trichoderma* spp. against fungal pathogens (e.g. Druzhinina et al. 2011). Chet et al. (1998) described four crucial steps during mycoparasitism: (1) chemotropism, (2) recognition, (3) attachment and coiling, and (4) lytic activity leading to death of the mycelium. In our in vitro experimental setup, the attachment, characterized by hyphal growth alongside the pathogen hyphae and appearance of specialized structures (i.e. papillae and hooks), and coiling previous to pathogen mycelial degradation were undoubtedly visualized. Papilla-like structures of *Trichoderma* spp. have been defined previously for other pathosystems (Lu et al. 2004; Druzhinina et al. 2011). These structures are similar to those reported in cucumber (Yedidia et al. 2000) and tomato roots (Chacón et al. 2007), identified as appressoria-like structures and analogous to the appressorium of plant pathogens (Druzhinina et al. 2011). Furthermore, *Trichoderma* can grow upon the prey and develop parasitic interactions developing hook-shape structures that are also involved in penetrating the host's mycelium by physical or chemical mechanisms (Lu et al. 2004; Brotman et al. 2010). Nonetheless, among all morphological features observed during the mycoparasitic interaction in *Trichoderma* spp., coiling is the most noteworthy. The capability of forming helix-shape hyphae around the pathogen, also present in other pathosystems (e.g. Lu et al. 2004), can also be key for a successful biological control effect. In the present study, these structures were observed clearly in vitro, wrapping *V. dahliae* hyphae. These microscopic events coincided with *V. dahliae* overgrowth by CECT 2413, an event usually associated with other mycoparasitic events (e.g. Ghanbarzadeh et al. 2014). However, there was no evidence of mycoparasitism in our *in planta* experiment, although we cannot completely rule out its occurrence on olive roots, nor exclude the presence of additional mechanisms among the battery of weapons this biocontrol fungus may deploy (Benítez et al. 2004). Chet et al. (1998) argued that parasitic interactions occur with less intensity *in planta* than in dual cultures due to a low nutrient concentration in soil if compared with the media.

The root colonization process by isolate CECT 2413, previously documented for herbaceous species (Chacón et al. 2007; Samolski et al. 2012; Alonso-Ramirez et al. 2014), has been elucidated here for olive. In this woody plant, CECT 2413 showed a high root colonization capability, as otherwise demonstrated for different isolates of *Trichoderma* spp. (Lu et al. 2004; Hohmann et al. 2011). Furthermore, *Th*-GFP was observed in the same spots as the pathogen. This fact could be essential for the success of biocontrol, as suggested by Kato et al. (2012). *Trichoderma* spp. are traditionally considered as fungi with high saprophytic and epiphytic activities, although usually limited to superficial layers when colonizing plant roots. Nevertheless, in some cases they can gain entrance to the plant interior (Harman et al. 2004). Endophytic lifestyle has thus been shown for several *Trichoderma* spp. isolates (Lu et al. 2004; Chacón et al. 2007; Hohmann et al. 2012). Unlike in the above-mentioned studies with herbaceous plants, there was no evidence for olive inner root colonization by CECT 2413.

In this study, CECT 2413 was inoculated as (pre-germinated) conidia suspensions. Hence, these structures were observed abundantly at early stages after inoculation. Furthermore, development of conidiophores was also observed *in planta* during the first sampling time points. However, both conidia and conidiophores gradually disappeared at later observation times, as previously reported (Bae and Knudsen 2000). This could be explained due to the fact that conidia can be highly sensitive to soil fungistasis

(Papavizas 1985). Overall, conidia usually show lower survival rate under natural conditions compared with other asexual propagules (Lewis and Papavizas 1983). Conidia were not the only propagule identified during the bioassays. Indeed, CECT 2413 developed a large number of chlamydospores. These resistant structures, previously identified/named as "yeast-like cells" by others (Chacón et al. 2007; Alonso-Ramirez et al. 2014), have been described for *Trichoderma* spp. in several environments such as liquid and solid media (Lewis and Papavizas 1983) or sterile natural and artificial soils (Park 1954). Papavizas (1985) suggested that production of chlamydospores can be related to a survival strategy of the fungus when introduced in natural ecosystems. The prevalence of resistance structures of *Trichoderma* could then be explained by nutrient shortage in the rhizosphere and the subsequent slow down of the BCA metabolism. Furthermore, Cohen et al. (1983) suggested that presence of organic/living matter such as plant tissues could favor chlamydospore formation and survival in soil. Thus, the overwhelming abundance of this resistant structure observed in our bioassays may be a consequence either of a normal behavior of this BCA in this particular niche or of a survival strategy due to adverse environmental conditions. So far, we do not have evidences supporting any of these two alternatives. Interestingly, chlamydospore formation took place under presence/absence of the pathogen. The production of an increasing number of chlamydospores on olive roots was concomitant with the progressive decrease of fluorescent hyphae that either eventually showed a substantial reduction (viz. *Th*-olive experiment) or a total absence at late observation times (viz. *Th*-olive-VDAT-36I experiment). While *Th*-GFP seemed to be absent at 17 DAI (no detectable fluorescent structures), viable CECT 2413 propagules were still present at the end of the *Th*-olive-VDAT-36I experiment as demonstrated by TSM quantification, although the BCA population size had decreased by two orders of magnitude regarding to the initial inoculum density. This fact together with the presence of chlamydospores after more than 100 days in *Th*-olive experiment confirmed the presence of this BCA in the olive rhizosphere, predominantly as resistant structure though. Therefore, we suggest a dormant state of the fungus in the form of chlamydospores in our experiments rather than loss of the inoculum. The way in which the BCA is applied can therefore determine its success in exerting biocontrol. Thus, when they are inoculated as conidia, chlamydospores or even at early conidia germination stages, their performance could be diminished because of the lack of nutrient sources. The likelihood of success would be enhanced when an adequate nutrients supply is added to the inocula (Yang et al. 2011). Pertot et al. (2008) stressed the importance that an adequate survival rate has for a successful biocontrol activity. The use of appropriate carriers is therefore a crucial factor when formulating and delivering BCA into a new environment. In this way, problems of inactivation, death and/or loss of biocontrol effectiveness of the BCA could be overcome (El-Hassan and Gowen 2006). Additionally, a regular supply of the BCA to maintain an adequate population level in the target niche could also be needed to counteract inoculum loss (Knudsen et al. 1991).

Few studies about the interaction of biocontrol fungi in plant roots by using advanced microscopy approaches are available (for instance, Zachow et al. 2010 and Kato et al. 2012). Recently, Lace et al. (2015) analysed, under in vitro culture conditions, the interactions between *Trichoderma atroviride* PKI1, two *Gigaspora* species and the herbaceous plant *Medicago truncatula* Gaertn. The same *Trichoderma* isolate used in the present study has been used in herbaceous species as well (Chacón et al. 2007; Samolski et al. 2012; Alonso-Ramirez et al. 2014). However, to the best of our knowledge, our work is the first one addressing the long-term colonization process of this BCA in a woody plant rhizosphere by CLSM that is, using living tissue. Moreover, we have been able to unravel the fate of the BCA biomass in this dynamic ecological niche over a long period of time, in the presence and absence of the target phytopathogen and under non-gnotobiotic conditions. Events here reported provide essential information (i.e. prevalence of chlamydospores) about the behavior of this BCA which can help to design more effective *Trichoderma*-based bioformulations. These bioformulations should be based on adequate carriers ensuring not only the activity of the BCA but also its durability.

Acknowledgments We are very grateful to M. N. Casa Adán for the help with CLSM at the University of Jaén facilities, and to M. Maldonado-González and A. Valverde-Corredor for their technical assistance. We appreciate the collaboration of NUTESCA SL in this project. This work was supported by

European Regional Development Fund-cofinanced grants from the Spanish Ministry of Economy and Competitiveness [Project number BIO2012-33904] and 'Junta de Andalucía' [Project number AGR-6038].

References

Aleandri MP, Chilosi G, Bruni N, Tomassini A, Vettraino AM, Vannini A (2015) Use of nursery potting mixes amended with local *Trichoderma* strains with multiple complementary mechanisms to control soil-borne diseases. Crop Prot 67:269–278

Alonso-Ramirez A, Poveda J, Martin I, Hermosa R, Monte E, Nicolas C (2014) Salicylic acid prevents *Trichoderma harzianum* from entering the vascular system of roots. Mol Plant Pathol 15(8):823–831

Askew DJ, Laing MD (1993) An adapted selective medium for the quantitative isolation of *Trichoderma* species. Plant Pathol 42(5):686–690

Bae YS, Knudsen GR (2000) Cotransformation of *Trichoderma harzianum* with beta-glucuronidase and green fluorescent protein genes provides a useful tool for monitoring fungal growth and activity in natural soils. Appl Environ Microbiol 66(2):810–815

Barroso Albarracín JB, Carreras Egaña A, Valderrama Rodríguez R, Chaki M, Begara Morales J, Mercado-Blanco J, Pérez Artés E, Rincón Romero A, Carballo Codón A, Benítez Fernández T, Valverde Corredor A, Guevara Pezoa F, Rodríguez Palero MJ, Dueñas Sánchez R, Fierro Risco J, López García A (2014) Cepa de *Trichoderma* útil para el tratamiento y/o prevención de infecciones provocadas por hongos pertenecientes al género *Verticilium*. Spanish Patent ES2393728

Benítez T, Rincón AM, Limón MC, Codón AC (2004) Biocontrol mechanisms of *Trichoderma* strains. Int Microbiol 7:249–260

Brotman Y, Kapuganti JG, Viterbo A (2010) *Trichoderma*. Curr Biol 20(9):R390–R391

Carvalho DDC, Lobo M, Martins I, Inglis PW, Mello SCM (2014) Biological control of *Fusarium oxysporum* f. sp *phaseoli* by *Trichoderma harzianum* and its use for common bean seed treatment. Trop Plant Pathol 39(5):384–391

Chacón MR, Rodríguez-Galán O, Benítez T, Sousa S, Rey M, Llobell A, Delgado-Jarana J (2007) Microscopic and transcriptome analyses of early colonization of tomato roots by *Trichoderma harzianum*. Int Microbiol 10(1):19–27

Chet I, Benhamou N, Haran S (1998) Mycoparasitism and lytic enzymes. In: Harman GE, Kubicek CP (eds) *Trichoderma & Gliocladium*. Enzymes, biological control and commercial applications, vol 2. Taylor and Francis Ltd, London, UK, pp 153–172

Cohen SD, Lewis JA, Papavizas GC, Bean GA (1983) Chlamydospore formation by *Trichoderma* spp. in organic-matter amended soil. Phytopathology 73(5):820

Contreras-Cornejo HA, Ortiz-Castro R, López-Bucio J (2013) Promotion of plant growth and the induction of systemic defence by *Trichoderma*: physiology, genetics and gene expression. In: Mukherjee PK, Horwitz BA, Singh US, Mukherjee M, Schmoll M (eds) *Trichoderma*: biology and applications. CABI, Walingford, UK, pp 173–194

Druzhinina IS, Seidl-Seiboth V, Herrera-Estrella A, Horwitz BA, Kenerley CM, Monte E, Mukherjee PK, Zeilinger S, Grigoriev IV, Kubicek CP (2011) *Trichoderma*: the genomics of opportunistic success. Nat Rev Microbiol 9(10):749–759

El-Hassan SA, Gowen SR (2006) Formulation and delivery of the bacterial antagonist *Bacillus subtilis* for management of lentil vascular wilt caused by *Fusarium oxysporum* f. sp *lentis*. J Phytopathol 154(3):148–155

Ghanbarzadeh B, Safaie N, Goltapeh EM (2014) Antagonistic activity and hyphal interactions of *Trichoderma* spp. against *Fusarium proliferatum* and *F. oxysporum in vitro*. Arch Phytopathol Plant Prot 47(16):1979–1987

Harman GE, Kubicek CP (1998) *Trichoderma & Gliocladium*: enzymes, biological control and commercial applications, vol 2. Taylor & Francis Ltd, London, UK

Harman GE, Howell CR, Viterbo A, Chet I, Lorito M (2004) *Trichoderma* species: opportunistic, avirulent plant symbionts. Nat Rev Microbiol 2(1):43–56

Hermosa R, Viterbo A, Chet I, Monte E (2012) Plant-beneficial effects of *Trichoderma* and of its genes. Microbiology 158:17–25

Hohmann P, Jones EE, Hill RA, Stewart A (2011) Understanding *Trichoderma* in the root system of *Pinus radiata*: associations between rhizosphere colonisation and growth promotion for commercially grown seedlings. Fungal Biol 115(8):759–767

Hohmann P, Jones EE, Hill RA, Stewart A (2012) Ecological studies of the bio-inoculant *Trichoderma hamatum* LU592 in the root system of *Pinus radiata*. FEMS Microbiol Ecol 80(3):709–721

Jiménez-Díaz RM, Trapero-Casas JL, Boned J, Landa del Castillo BB, Navas-Cortés JA (2009) Uso de Bioten para la protección biológica de plantones de olivo contra la Verticilosis causada por el patotipo defoliante de *Verticillium dahliae*. Bol San Veg. Plagas, 35:595–615 (with an abstract in English)

Kato A, Miyake T, Nishigata K, Tateishi H, Teraoka T, Arie T (2012) Use of fluorescent proteins to visualize interactions between the Bakanae disease pathogen *Gibberella fujikuroi* and the biocontrol agent *Talaromyces* sp KNB-422. J Gen Plant Pathol 78(1):54–61

Knudsen GR, Eschen DJ, Dandurand LM, Bin L (1991) Potential for biocontrol of *Sclerotinia sclerotiorum* through colonization of sclerotia by *Trichoderma harzianum*. Plant Dis 75:466–470

Kredics L, Hatvani L, Naeimi S, Körmöczi P, Manczinger L, Vágvölgyi C, Druzhinina I (2014) Chapter 1: biodiversity of the genus *Hypocrea/Trichoderma* in different habitats. In: Gupta VK, Schmoll M, Herrera-Estrella A, Upadhyay RS, Druzhinina I, Tuohy M (eds) Biotechnology and biology of *Trichoderma*. Elsevier, Amsterdam, The Netherlands, pp 3–24

Lace B, Genre A, Woo S, Faccio A, Lorito M, Bonfante P (2015) Gate crashing arbuscular mycorrhizas: *in vivo* imaging shows the extensive colonization of both symbionts by *Trichoderma atroviride*. Env Microbiol Rep 7(1):64–77

Lewis JA, Papavizas GC (1983) Production of chlamydospores and conidia by *Trichoderma* spp in liquid and solid growth media. Soil Biol Biochem 15(3):351–357

López-Escudero FJ, Mercado-Blanco J (2011) Verticillium wilt of olive: a case study to implement an integrated strategy to control a soil-borne pathogen. Plant Soil 344(1):1–50

López-Escudero FJ, del Río C, Caballero JM, Blanco-López MA (2004) Evaluation of olive cultivars for resistance to *Verticillium dahliae*. Eur J Plant Pathol 110(1):79–85

Lorito M, Woo S (2015) *Trichoderma*: A multi-purpose tool for integrated pest management. In: Lugtenberg B (ed) Principles of plan-microbe interactions. Microbes Sustain Agric, Springer, USA, pp 345–353

Lu ZX, Tombolini R, Woo S, Zeilinger S, Lorito M, Jansson JK (2004) In vivo study of *Trichoderma*-pathogen-plant interactions, using constitutive and inducible green fluorescent protein reporter systems. Appl Environ Microbiol 70(5):3073–3081

Mercado-Blanco J, Rodríguez-Jurado D, Hervás A, Jiménez-Diaz RM (2004) Suppression of verticillium wilt in olive planting stocks by root-associated fluorescent *Pseudomonas* spp. Biol Control 30(2):474–486

Moreno-Mateos MA, Delgado-Jarana J, Codón AC, Benítez T (2007) pH and Pac1 control development and antifungal activity in *Trichoderma harzianum*. Fungal Genet Biol 44(12):1355–1367

Papasotiriou FG, Varypatakis KG, Christofi N, Tjamos SE, Paplomatas EJ (2013) Olive mill wastes: a source of resistance for plants against *Verticillium dahliae* and a reservoir of biocontrol agents. Biol Control 67(1):51–60

Papavizas GC (1985) *Trichoderma* and *Gliocladium*- biology, ecology, and potential for biocontrol. Annu Rev Phytopathol 23:23–54

Park D (1954) Chlamydospores and survival in soil fungi. Nature 173:454–455

Pegg GF, Brady BL (2002) Verticillium wilts. CAB International, Wallingford, UK

Penttilä M, Nevalainen H, Rättö M, Salminen E, Knowles J (1987) A versatile transformation system for the cellulolytic filamentous fungus *Trichoderma reesei*. Gene 61(2):155–164

Pertot I, Gobbin D, De Luca F, Prodorutti D (2008) Methods of assessing the incidence of Armillaria root rot across viticultural areas and the pathogen's genetic diversity and spatial–temporal pattern in northern Italy. Crop Prot 27(7):1061–1070

Prieto P, Navarro-Raya C, Valverde-Corredor A, Amyotte SG, Dobinson KF, Mercado-Blanco J (2009) Colonization process of olive tissues by *Verticillium dahliae* and its *in planta* interaction with the biocontrol root endophyte *Pseudomonas fluorescens* PICF7. Microb Biotechnol 2(4):499–511

Raaijmakers JM, Paulitz TC, Steinberg C, Alabouvette C, Moenne-Loccoz Y (2009) The rhizosphere: a playground and battlefield for soilborne pathogens and beneficial microorganisms. Plant Soil 321(1–2):341–361

Rincón AM, Chaki M, Fierro-Risco J, Valverde-Corredor A, Carreras A, Pérez-Artés E, Begara JC, Valderrama R, Barroso JB, Mercado-Blanco J (2014) Biological control of Verticillium wilt of olive by *Trichoderma harzianum*. In: XII Meeting of the IOBC/WPRS Working Group, Biological control of fungi and bacterial plant pathogens. Upsala, Sweden, p 78

Ruano-Rosa D, del Moral-Navarrete L, Lopez-Herrera CJ (2010) Selection of *Trichoderma* spp. isolates antagonistic to *Rosellinia necatrix*. Span J Agric Res 8(4):1084–1097

Ruano-Rosa D, Cazorla FM, Bonilla N, Martín-Pérez R, De Vicente A, López-Herrera CJ (2014) Biological control of avocado white root rot with combined applications of *Trichoderma* spp. and rhizobacteria. Eur J Plant Pathol 138(4):751–762

Samolski I, Rincón AM, Pinzón LM, Viterbo A, Monte E (2012) The qid74 gene from *Trichoderma harzianum* has a role in root architecture and plant biofertilization. Microbiol-SGM 158(1):129–138

Tjamos EC (1993) Prospects and strategies in controlling Verticillium wilt of olive. EPPO Bull 23(3):505–512

Verma M, Brar SK, Tyagi RD, Surampalli RY, Valéro JR (2007) Antagonistic fungi, *Trichoderma* spp.: panoply of biological control. Biochem Eng J 37(1):1–20

Vitullo D, Altieri R, Esposito A, Nigro F, Ferrara M, Alfano G, Ranalli G, De Cicco V, Lima G (2013) Suppressive biomasses and antagonist bacteria for an eco-compatible control of *Verticillium dahliae* on nursery-grown olive plants. Int J Environ Sci Technol 10(2):209–220

Yang XM, Chen LH, Yong XY, Shen QR (2011) Formulations can affect rhizosphere colonization and biocontrol efficiency of *Trichoderma harzianum* SQR-T037 against Fusarium wilt of cucumbers. Biol Fertil Soils 47(3):239–248

Yedidia I, Benhamou N, Kapulnik Y, Chet I (2000) Induction and accumulation of PR proteins activity during early stages of root colonization by the mycoparasite *Trichoderma harzianum* strain T-203. Plant Physiol Biochem 38(11):863–873

Zachow C, Fatehi J, Cardinale M, Tilcher R, Berg G (2010) Strain-specific colonization pattern of *Rhizoctonia* antagonists in the root system of sugar beet. FEMS Microbiol Ecol 74(1):124–135

David Ruano-Rosa is a postdoctoral researcher skilled on integrated control of soil-borne pathogens of woody plants, on the selection and characterization of biological control agents with special interest in the genera *Trichoderma* and *Pseudomonas*, and on the study of phytopathogen-biological control agent interactions.

Pilar Prieto is interested in the analysis of genome organization in cereals, particularly rice and wheat, combining confocal microscopy with genomic and proteomic approaches. The study of chromosome associations during meiosis is a relevant research topic. She aims to transfer agronomic traits into wheat by manipulating chromosome associations to promote interspecific recombination between wheat and related species such as wild and cultivated barley. The study of the colonization processes of cereals and olive tissues by microorganisms using confocal microscopy is another research area.

Ana María Rincón is researcher and lecturer at the University of Seville, Spain. Her work has been focused on molecular genetics and improvement of strains of *Trichoderma* spp. as biological control agents since 1997. She has taken part in numerous projects to develop *Trichoderma*-based formulations for crop protection.

María Victoria Gómez-Rodríguez is lecturer in plant physiology at the Universidad de Jaén, Spain, since 23 years ago. Her main research interests are plant-pathogen interaction and plant induced resistance mechanisms against oomycetes.

Raquel Valderrama is professor in Biochemistry and Molecular Biology and her investigation is focused on the study of the response of antioxidant systems and several reactive oxygen and nitrogen species (ROS and RNS) in plants during development and biotic/abiotic stress conditions.

Juan Bautista Barroso is full professor of Biochemistry and Molecular Biology and his research is focused on the study of the metabolism of several reactive oxygen and nitrogen species (ROS and RNS) and their implications on the plant defense mechanisms against different biotic and abiotic stress conditions.

Jesús Mercado-Blanco is tenured scientist in the Institute for Sustainable Agriculture (Spanish National Research Council, CSIC). His main research interests focus on agricultural microbiology and biotechnology and the development of control tools within integrated disease management strategies, using Verticillium wilt of olive as study model. Specific research topics are the bases underlying plant–microbe interactions by molecular and '-omic' approaches and the identification, characterization and use of microbiological control agents, with emphasis on bacterial endophytes.